

# Vibration Testing for Anomaly Detection

Habib Ammari\*    Hyeonbae Kang<sup>†</sup>    Eunjoo Kim<sup>†</sup>    Hyundae Lee<sup>‡</sup>

November 26, 2007

## Abstract

In this paper we propose an efficient method to reconstruct a small inclusion buried inside a body using the perturbation of modal parameters measured on the boundary of the body. We design a reconstruction algorithm based on the asymptotic expansions of the eigenvalue perturbations obtained by Ammari and Moskow in [9]. We then implement this algorithm and demonstrate its viability and limitations.

**AMS subject classifications.** 35R30, 35B34

**Key words.** anomaly detection, vibration analysis, asymptotic expansion, reconstruction algorithm

## 1 Introduction

This paper is concerned with detection of diametrically small inclusions buried inside a body by means of boundary measurements. Since the pioneer work of Friedman and Vogelius [13], detection of small inclusions has been one of the central problems in electrical impedance tomography (EIT). EIT uses the current-voltage measurements to reconstruct the conductivity distribution. This method has been applied to detect elastic inclusions using the traction-displacement measurements on the boundary [8, 16]. We refer the readers to the recent books [3, 4] for recent developments in impedance imaging of small inclusions.

In this paper we develop a numerical method to reconstruct small inclusions using the perturbation of modal parameters. If there is a small inclusion inside a body, then the eigenvalues and corresponding eigenfunctions of the body are perturbed. The problem to be considered in this paper is to detect the location and estimate the size of the inclusion using these perturbations.

To be more precise, let  $\Omega$  be a domain in  $\mathbb{R}^d$ ,  $d = 2, 3$ , with a connected  $\mathcal{C}^2$  boundary. The domain  $\Omega$  represents a body which contains an inclusion. We consider the eigenvalue problem (in the absence of the inclusion) for the Laplacian with the Neumann boundary condition:

$$\begin{cases} \Delta v_0 + \omega_0^2 v_0 = 0 & \text{in } \Omega, \\ \frac{\partial v_0}{\partial \nu} = 0 & \text{on } \partial\Omega, \end{cases} \quad (1.1)$$

---

\*Laboratoire Ondes et Acoustique, CNRS & ESPCI, 10 rue Vauquelin, 75231 Paris Cedex 05, France (habib.ammari@espci.fr).

<sup>†</sup>School of Mathematical Sciences, Seoul National University, Seoul 151-747, Korea (hkang@math.snu.ac.kr, kej@math.snu.ac.kr).

<sup>‡</sup>Centre de Mathématiques Appliquées, Ecole Polytechnique, 91128 Palaiseau Cedex, France (lee@cmapx.polytechnique.fr).

where  $v_0$  is normalized so that  $\|v_0\|_{L^2(\Omega)} = 1$ . Throughout this paper, we assume for the sake of clarity that  $\omega_0$  is simple.

Suppose that  $\Omega$  contains a small inclusion  $D$  of the form

$$D = z + \epsilon B, \quad (1.2)$$

where  $B$  is a bounded domain containing the origin which plays the role of a reference domain,  $\epsilon$  is a small parameter (the characteristic size of the inclusion), and  $z$  indicates the location of the inclusion. We also assume that  $|B| = 1$ . We suppose the material parameter of  $D$  is  $k \neq 1$  while that of the background  $\Omega \setminus D$  is 1. Due to presence of the inclusion  $D$  the eigenvalue and eigenfunction of the body  $\Omega$  are perturbed, and perturbed ones satisfy the following eigenvalue problem:

$$\begin{cases} \nabla \cdot (1 + (k-1)\chi_D)\nabla v_\epsilon + \omega_\epsilon^2 v_\epsilon = 0 & \text{in } \Omega, \\ \frac{\partial v_\epsilon}{\partial \nu} = 0 & \text{on } \partial\Omega, \end{cases} \quad (1.3)$$

with  $\|v_\epsilon\|_{L^2(\Omega)} = 1$ , where  $\chi_D$  denotes the characteristic function of  $D$ .

The aim of this work is to detect the small inclusion  $D$ , in particular, its location  $z$  and its size, from variations of the modal parameters

$$\left( \omega_\epsilon - \omega_0, (v_\epsilon - v_0)|_{\Gamma_\epsilon} \right). \quad (1.4)$$

Difficulties of this inverse problem result from its inherent ill-posedness and nonlinearity. Many authors have proposed various reconstruction algorithms, most of which are based on laborious least-square algorithms and Newton-type iteration schemes.

In this paper, our basic ingredient in detecting the inclusion  $D$  is an asymptotic formula for the perturbation  $\omega_\epsilon - \omega_0$  obtained by Ammari and Moskow [9]:

$$\omega_\epsilon^2 - \omega_0^2 = \epsilon^d M \nabla v_0(z) \cdot \nabla v_0(z) + O(\epsilon^{d+1}), \quad (1.5)$$

as  $\epsilon \rightarrow 0$ , where  $M = M(k, B)$  is the polarization tensor (PT) associated with  $B$  and  $k$ . (See the beginning of the next section for the notion of PT.) See [7] for derivation of a complete asymptotic expansion of  $\omega_\epsilon^2 - \omega_0^2$ . It is well-known from the perturbation theory of linear operators [19] that

$$\|v_\epsilon - v_0\|_{L^2(\Omega)} \rightarrow 0, \quad (1.6)$$

as  $\epsilon \rightarrow 0$ . Using the leading-order term in (1.5) and (1.6) we derive a functional whose minimizer provides us with information on the location and the size of the inclusion.

Note that in view of the first equation in (1.3) the boundary conditions on  $\partial D$  is given by the transmission conditions. It is worthwhile mentioning that the method of this paper can be applied to situations with different types of boundary conditions. For example, if the Dirichlet boundary condition is imposed on the boundary of the inclusion, then the asymptotic formula for the eigenvalue perturbation has been derived in [7] (see also [10, 23, 24, 25]). In a similar way to this paper, one can use this formula to detect the location and the capacity (instead of the polarization tensor) of the inclusion. One can also use the asymptotic formula for the eigenvalue perturbation for the elasticity problem in [6] to detect an elastic inclusion. A similar method has been employed to detect internal corrosive parts of small Hausdorff measure in a two-dimensional structure [5].

This paper is organized as follows. In the next section we derive a functional whose minimizer yields the location and size of the inclusion. In section 3, we perform numerical experiments to test the viability of the algorithm.

## 2 Reconstruction of an inclusion

Let us begin this section with a brief review of the notion of the polarization tensor. For a given domain  $B$  with Lipschitz boundary (not necessarily connected), the PT  $M = M(B) = (m_{ij})_{i,j=1}^d$  associated with  $B$  is defined to be

$$m_{ij} = (k-1) \int_{\partial B} \psi_i \frac{\partial x_j}{\partial \nu} d\sigma \quad (2.1)$$

where  $\psi_i$  is the solution to

$$\begin{cases} \nabla \cdot (1 + (k-1)\chi_B)\nabla \psi_i = 0 & \text{in } \mathbb{R}^d, \\ \psi_i(x) - x_i = O(|x|^{1-d}) & \text{as } |x| \rightarrow \infty. \end{cases} \quad (2.2)$$

See, for example, [4, page 77]. It is worth noticing that  $\epsilon^d M(B)$  is the PT for  $D = z + \epsilon B$ , which can be seen easily by scaling.

The notion of PT appears in the theory of composites as the low-volume fraction limit of the effective conductivity. It also occurs in a very promising asymptotic approach for imaging small inclusions. See [3, 4, 22] and the references therein for both of these applications.

In view of its connection to the theory of composites, it is natural for the PT to have the following bounds, which are called the Hashin-Shtrikman (HS) bounds after the names of scientists who found optimal bounds for the effective conductivity [14].

If  $B$  is a domain with  $|B| = 1$ , then the PT associated with  $B$  satisfies

$$\text{Trace}(M) < (k-1)(d-1 + \frac{1}{k}), \quad (2.3)$$

and

$$\text{Trace}(M^{-1}) \leq \frac{d-1+k}{k-1}. \quad (2.4)$$

These bounds were obtained in [21, 12], and proved to be optimal in [12, 2].

If  $B$  is an ellipse of the form  $R(B')$  where  $R$  is a rotation by  $\theta$  and  $B'$  is an ellipse of the form  $\frac{x^2}{a^2} + \frac{y^2}{b^2} \leq 1$ , then it is known (see [4, page 81 & page 122] for example) that its PT is given by

$$M(B) = (k-1)R \begin{pmatrix} \frac{a+b}{a+kb} & 0 \\ 0 & \frac{a+b}{a+kb} \end{pmatrix} R^T. \quad (2.5)$$

Thus for a given PT there corresponds a unique ellipse whose PT is the given one [11]. It is worth mentioning that the PT for the ellipses (or ellipsoids) satisfy the lower HS-bound (2.4). Recently, the converse was proved to be true, as an immediate consequence of which the Pólya-Szegő conjecture follows [17, 18].

We now derive a method of reconstruction. Suppose that  $\omega_0$  is a simple eigenvalue of (1.1) and  $v_0$  to be the (normalized) associated eigenfunction. Note that the eigenvalues of (1.3) are generically simple [1, 26].

For  $h \in L^2(\partial\Omega)$  satisfying  $\int_{\partial\Omega} h v_0 = 0$ , let  $w_h$  be the solution to

$$\begin{cases} (\Delta + \omega_0^2)w_h = 0 & \text{in } \Omega, \\ \frac{\partial w_h}{\partial \nu} = h & \text{on } \partial\Omega. \end{cases} \quad (2.6)$$

Existence and uniqueness of a solution to (2.6) are guaranteed by the orthogonality condition  $\int_{\partial\Omega} h v_0 = 0$ . Equation (1.3) says that the following transmission condition holds along the interface  $\partial D$ :

$$\frac{\partial v_\epsilon}{\partial \nu} \Big|_+ = k \frac{\partial v_\epsilon}{\partial \nu} \Big|_-, \quad (2.7)$$

where the subscripts  $\pm$  indicate the limit from outside and inside  $D$ , respectively. By integration by parts, it then follows that

$$\begin{aligned} (\omega_\epsilon^2 - \omega_0^2) \int_{\Omega \setminus D} v_\epsilon w_h &= - \int_{\Omega \setminus D} \Delta v_\epsilon w_h + \int_{\Omega \setminus D} v_\epsilon \Delta w_h \\ &= \int_{\partial\Omega} h v_\epsilon - \int_{\partial D} \left( v_\epsilon \frac{\partial w_h}{\partial \nu} - w_h \frac{\partial v_\epsilon}{\partial \nu} \Big|_+ \right) \\ &= \int_{\partial\Omega} h v_\epsilon - \int_{\partial D} \left( v_\epsilon \frac{\partial w_h}{\partial \nu} - k w_h \frac{\partial v_\epsilon}{\partial \nu} \Big|_- \right) \\ &= \int_{\partial\Omega} h v_\epsilon + (k-1) \int_D \nabla v_\epsilon \cdot \nabla w_h - (\omega_\epsilon^2 - \omega_0^2) \int_D v_\epsilon w_h. \end{aligned}$$

Thus we have

$$(\omega_\epsilon^2 - \omega_0^2) \int_\Omega v_\epsilon w_h = \int_{\partial\Omega} h v_\epsilon + (k-1) \int_D \nabla v_\epsilon \cdot \nabla w_h. \quad (2.8)$$

It is also proved in [9] that the following inner expansion for the (normalized) eigenfunction  $v_\epsilon$  holds for  $x$  near  $z$ :

$$v_\epsilon(x) = v_0(z) + \epsilon \sum_{j=1}^d \partial_j v_0(z) \psi_j \left( \frac{x-z}{\epsilon} \right) + o(\epsilon). \quad (2.9)$$

Since  $w_h$  is smooth in  $\Omega$ , it follows from (2.9) that

$$\begin{aligned} \int_D \nabla v_\epsilon \cdot \nabla w_h dx &= \int_D \nabla v_\epsilon dx \cdot \nabla w_h(z) + O(\epsilon^{d+1}) \\ &= \int_{\partial D} v_\epsilon \nu d\sigma \cdot \nabla w_h(z) + O(\epsilon^{d+1}) \\ &= \int_{\partial D} \left[ \epsilon \sum_{j=1}^d \partial_j v_0(z) \psi_j \left( \frac{x-z}{\epsilon} \right) + o(\epsilon) \right] \nu d\sigma \cdot \nabla w_h(z) + O(\epsilon^{d+1}). \end{aligned}$$

After an obvious change of variables, we now obtain from (2.1) that the following expansion holds:

$$(k-1) \int_D \nabla v_\epsilon \cdot \nabla w_h = \epsilon^d M \nabla v_0(z) \cdot \nabla w_h(z) + o(\epsilon^d). \quad (2.10)$$

Substituting (2.10) into (2.8) yields

$$(\omega_\epsilon^2 - \omega_0^2) \int_{\Omega} v_\epsilon w_h = \int_{\partial\Omega} h v_\epsilon + \epsilon^d M \nabla v_0(z) \cdot \nabla w_h(z) + o(\epsilon^d). \quad (2.11)$$

Dividing both sides of (2.11) by  $\omega_\epsilon^2 - \omega_0^2$  and using (1.5), we arrive at

$$\frac{M \nabla v_0(z) \cdot \nabla w_h(z)}{M \nabla v_0(z) \cdot \nabla v_0(z)} = -\frac{1}{\omega_\epsilon^2 - \omega_0^2} \int_{\partial\Omega} h v_\epsilon d\sigma + \int_{\Omega} v_\epsilon w_h dx + o(1).$$

Since  $\int_{\partial\Omega} h v_0 = 0$ , we conclude from (1.6) that

$$\frac{M \nabla v_0(z) \cdot \nabla w_h(z)}{M \nabla v_0(z) \cdot \nabla v_0(z)} = -\frac{1}{\omega_\epsilon^2 - \omega_0^2} \int_{\partial\Omega} h(v_\epsilon - v_0) d\sigma + \int_{\Omega} v_0 w_h dx + o(1). \quad (2.12)$$

We emphasize that the right-hand side of (2.12) can be computed using modal measurements (1.4).

In view of (2.12), the reconstruction method is rather obvious. With the measurements (1.4) and a finite number of linearly independent functions  $h_1, \dots, h_l$ , on  $\partial\Omega$  satisfying  $\int_{\partial\Omega} h_j v_0 d\sigma = 0$ , define the functional  $J$  by

$$J(x, M) := \sum_{j=1}^{\ell} \left| \frac{M \nabla v_0(x) \cdot \nabla w_{h_j}(x)}{M \nabla v_0(x) \cdot \nabla v_0(x)} + \frac{1}{\omega_\epsilon^2 - \omega_0^2} \int_{\partial\Omega} h_j(v_\epsilon - v_0) - \int_{\Omega} v_0 w_{h_j} \right|^2 \quad (2.13)$$

for  $x \in \Omega$  and  $M$  the polarization tensor associated with the domain  $B$  satisfying  $|B| = 1$ . The method for detecting the inclusion is to minimize

$$\min_{x, M} J(x, M), \quad (2.14)$$

where the minimization is done over  $x \in \Omega$  and  $M$  satisfying the bounds (2.3) and (2.4). Once  $z$  and  $M$  were found, the size  $|D| = \epsilon^d$  of the inclusion can be computed using (1.5).

Note that the dependence of the functional  $J$  with respect the reference domain  $B$  is only through the polarization tensor. This means that it is not possible to distinguish those domains which have the same PTs. Thus we only consider the class of ellipses or ellipsoids which have one-to-one correspondence with the class of PTs. For example, if  $B$  is an ellipse then its PT takes the form

$$M = R \begin{pmatrix} \lambda & 0 \\ 0 & \mu \end{pmatrix} R^T, \quad (2.15)$$

where

$$\lambda = (k-1) \frac{a+b}{a+kb}, \quad \frac{1}{\lambda} + \frac{1}{\mu} = \frac{k+1}{k-1},$$

and  $R$  is a rotation, say  $R = \begin{pmatrix} \cos \theta & -\sin \theta \\ \sin \theta & \cos \theta \end{pmatrix}$  for  $\theta \in [0, \pi)$ . Therefore, the functional  $J$  can be rewritten as

$$J(x, \theta, \lambda) := \sum_{j=1}^{\ell} \left| \frac{M \nabla v_0(x) \cdot \nabla w_{h_j}(x)}{M \nabla v_0(x) \cdot \nabla v_0(x)} + \frac{1}{\omega_\epsilon^2 - \omega_0^2} \int_{\partial\Omega} h_j(v_\epsilon - v_0) - \int_{\Omega} v_0 w_{h_j} \right|^2, \quad (2.16)$$

where the variables run over  $x \in \Omega$ ,  $0 \leq \theta < \pi$ , and  $\frac{k-1}{k} \leq \lambda < k-1$  according to the HS-bounds (2.3) and (2.4).

In summary, the reconstruction procedure is as follows.

**[Reconstruction by Vibration]**

- Step 1. [Location Direction] Minimize  $J(x, \theta, \lambda)$  to detect the location  $z$  and the PT  $M$  of  $B$ .  
 Step 2. [Size Direction] Use (1.5) to estimate the characteristic size  $\epsilon$  of the inclusion.

### 3 Numerical results

We now present some results of numerical experiments to demonstrate the viability of our reconstruction algorithm. We first explain how we acquire the data for simulation and test functions, and then describe the minimization procedure employed for computation.

**Data acquisition.** We first explain how we acquire the modal parameters  $\omega_\epsilon - \omega_0$  and  $v_\epsilon - v_0$  on  $\partial\Omega$ . In the following,  $\Omega$  is assumed to be the ellipse of the form:

$$\frac{x^2}{a^2} + \frac{y^2}{b^2} \leq 1, \quad a = 1, \quad b = 0.95. \quad (3.1)$$

The reason for taking  $\Omega$  as an ellipse instead of a disk is that the first Neumann eigenvalue for the disk is not simple. We then compute the first eigenvalue of (1.1),  $\omega_0$ , using the PDE-tool of MATLAB. The (normalized) eigenvector  $v_0$  in  $\Omega$  can be computed using the same tool. But, in order to have discrete grid points of  $\Omega$  at our disposal, we first compute  $v_0|_{\partial\Omega}$  using MATLAB, and then compute the interior values of  $v_0$  using the double-layer potential, namely,

$$v_0(x) = c\mathcal{D}_\Omega^{\omega_0}[v_0](x), \quad x \in \Omega, \quad (3.2)$$

where the constant  $c$  is for normalization. For the double-layer potential for the Helmholtz operator, we refer to [7] for example. As results of computation we obtain  $\omega_0 = 1.8449$  and Figure 1 for  $v_0$ . The left two diagrams in Figure 1 show  $v_0$  in  $\Omega$  from two different views. The plot in the right-hand side is the graph of  $|\nabla v_0(x)|$  in  $\Omega$ . We emphasize that  $|\nabla v_0(x)|$  does not vanish in  $\Omega$ . In fact, we known from [15, Theorem 1.4] that, in two dimensions, the gradient of the first Neumann eigenfunction does not vanish in the domain as long as the domain is convex and is symmetric with respect to both coordinate axes.

If the inclusion  $D$  takes an elliptic shape, then we can compute the eigenvalue  $\omega_\epsilon$  and the eigenfunction  $v_\epsilon$  of (1.3) using the same PDE-tool of MATLAB. For inclusions of shapes other than ellipses, we take as the eigenvalue the leading-order term in (1.5), *i.e.*,

$$\omega_\epsilon^2 = \omega_0^2 + \epsilon^d M \nabla v_0(z) \cdot \nabla v_0(z). \quad (3.3)$$

In the case of elliptic inclusions, the above formula is in a good match with the eigenvalue computed by MATLAB if  $\epsilon$  is small. For the eigenfunction  $v_\epsilon$  we solve (1.3) using the boundary integral method based on the layer potentials. We refer to [7] for the computation of the eigenfunction using layer potentials.

**Test functions.** For the test functions  $w_h$  for (2.6), we take the following  $h$ :

$$h_j(\theta) = a_1 \cos \theta + a_{j+1} \cos(j+1)\theta, \quad (\cos \theta, 0.95 \sin \theta) \in \partial\Omega, \quad j = 1, 2, \dots, \ell$$

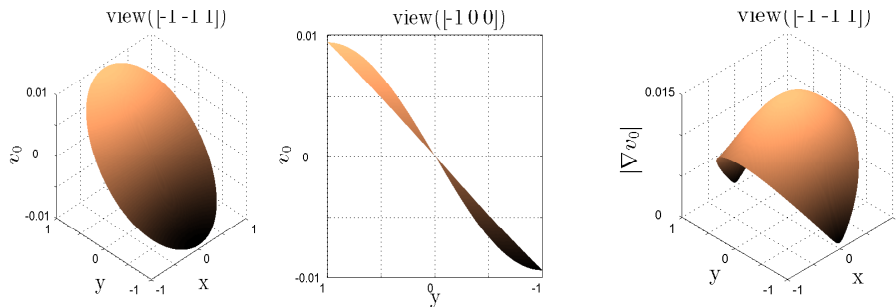


Figure 1: The two left-hand plots are  $v_0$  from different viewpoints. The right-hand plot is  $|\nabla v_0|$  in the case where the domain  $\Omega$  is an ellipse.

where the constants  $a_1$  and  $a_{j+1}$  are taken so that  $\int_{\partial\Omega} h_k v_0 = 0$ . We use  $\ell = 5$ . Then the corresponding solution  $w_{h_j}$  is computed using the boundary integral method again.

**Minimization procedure.** We first note that the variables  $(x, \theta, \lambda)$  for the functional  $J$  runs over

$$K := \Omega \times [0, 2\pi) \times \left[ \frac{k-1}{k}, k-1 \right). \quad (3.4)$$

Probably the easiest way to minimize  $J$  on  $K$  is to divide  $K$  into small meshes and to compute  $J$  on nodal points. This works well if  $k$  is close to 1. But if  $k$  is very large or close to 0, then the interval  $[\frac{k-1}{k}, k-1)$  is too long and hence this straightforward method does not work so well. Moreover, we also deal with the case when  $k$  is not known *a priori*. In this case we set the computed material parameter  $k^c$  to be  $+\infty$  if  $\omega_\epsilon^2 - \omega_0^2 > 0$  and 0 otherwise, since the PT  $M$  is positive-definite if  $k > 1$  and negative-definite if  $k < 1$  [4, Theorem 4.11]. Therefore, in the case when exact  $k$  is not known, the variable  $\lambda$  runs over either  $[0, \infty)$  or  $(-\infty, 0]$ , and hence dividing this interval into meshes does not work.

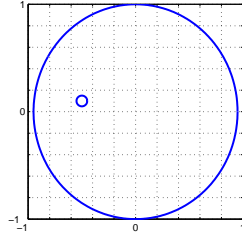
For these reasons, we use the Levenberg-Marquardt method to minimize  $J$ . The Levenberg-Marquardt method is a modified Newton type iteration method for the least-square problem. We refer to [20] for details of this method. In order for the iteration process to converge fast, it is necessary to have a good initial guess. For the purpose of having a good initial guess, we first assume that the PT  $M$  is a constant multiple of the identity matrix ( $= cI$ ), which amounts to assuming that the inclusion takes the shape of a disk, and minimize

$$J^d(x) := J(x, cI) = \sum_{j=1}^{\ell} \left| \frac{\nabla v_0(x) \cdot \nabla w_{h_j}(x)}{\nabla v_0(x) \cdot \nabla v_0(x)} + \frac{1}{\omega_\epsilon^2 - \omega_0^2} \int_{\partial\Omega} h_j (v_\epsilon - v_0) - \int_{\Omega} v_0 w_h \right|^2, \quad (3.5)$$

where  $x \in \Omega$ . The minimizer  $x_0$  of  $J^d$  is obtained by evaluating  $J^d$  at grid points of  $\Omega$ . Once the minimizer  $x_0 \in \Omega$  of  $J^d$  is obtained, we apply Levenberg-Marquardt iteration to  $J(x, \theta, \lambda)$ , with the initial guess  $x = x_0$ ,  $\theta = 0$ , and  $\lambda = \frac{2(k-1)}{k+1}$ , until the minimal values of  $J(x)$  stabilize. Note that if  $k$  is unknown, we take, as an initial guess for  $\lambda$ ,  $\lambda = 2$  if  $\omega_\epsilon^2 > \omega_0^2$  and  $\lambda = 2$  if  $\omega_\epsilon^2 < \omega_0^2$ .

We now present some results of numerical simulations.

**Example 1** [circular inclusion]. We test the reconstruction method to find a circular inclusion (of radius 0.05) with different material parameters  $k = 3, 10, 50, 100, 500$ . The upper plot in Figure 2 is the actual configuration with the inclusion. The upper half of the table in the same figure shows the computational results when  $k$  is known, while the lower one shows the results when  $k$  is unknown. In this case, since  $w_\epsilon - w_0 > 0$ , we take  $k = k^c = \infty$ . In the table,  $D^c$  is the detected ellipse centered at  $z^c$  with semi-lengths  $a^c$  and  $b^c$ , and the rotation  $\theta^c$ .



$k$	$z$	$r$	$k^c$	$a$	$b$	$ z - z^c $	$  D  -  D^c  $
3	(-0.5, 0.1)	0.05	3	5.4952e-2	4.7143e-2	1.8630e-3	2.8456e-4
10			5.0500e-2	4.9685e-2	1.4874e-3	2.8570e-5	
50			5.1847e-2	4.9296e-2	1.4376e-3	1.7539e-4	
100			5.7513e-2	4.7511e-2	3.2770e-3	7.3041e-4	
500			5.0735e-2	4.9674e-2	1.4279e-3	6.3502e-5	
3			$\infty$	3.5686e-2	3.4275e-2	1.8632e-3	4.0114e-3
10			$\infty$	4.5616e-2	4.3979e-2	1.4874e-3	1.5515e-3
50			$\infty$	5.2249e-2	4.7892e-2	1.4376e-3	7.3078e-6
100			$\infty$	5.0982e-2	4.8949e-2	1.4325e-3	1.4054e-5
500			$\infty$	7.5707e-2	4.2182e-2	1.4279e-3	2.1786e-3

Figure 2: Reconstruction results when the inclusion is a disk. The upper table shows the results in case when the material parameter  $k$  are known while the lower one is for the case when  $k$  is not known.

**Example 2** [elliptic inclusion]. We test the algorithm to find an inclusion of elliptic shape. As before, the upper part of the table in Figure 4 is for the case when  $k$  is known and the lower one is for the case when  $k$  is unknown. When  $k$  is known, the algorithm detects the location and shape pretty well. But when  $k$  is not known, the detected shape is a little tilted while the location is detected well.

**Example 3** [General-shape inclusion]. Figures 4, 5 and 6 show the computational results when the inclusion takes arbitrary shape.

**Example 4** [inclusion with non-small size]. We test the reconstruction method for an inclusion whose size is *not* small. In this example, the inclusion  $D$  is an ellipse with  $|D| = 4.7299e - 2$ . Figure 7 shows that the performance of the reconstruction method is pretty poor, which indicates that the algorithm is sensitive to the size (or diameter) of the inclusion. This is somewhat expected since our algorithm is based on the small volume expansion (1.5).

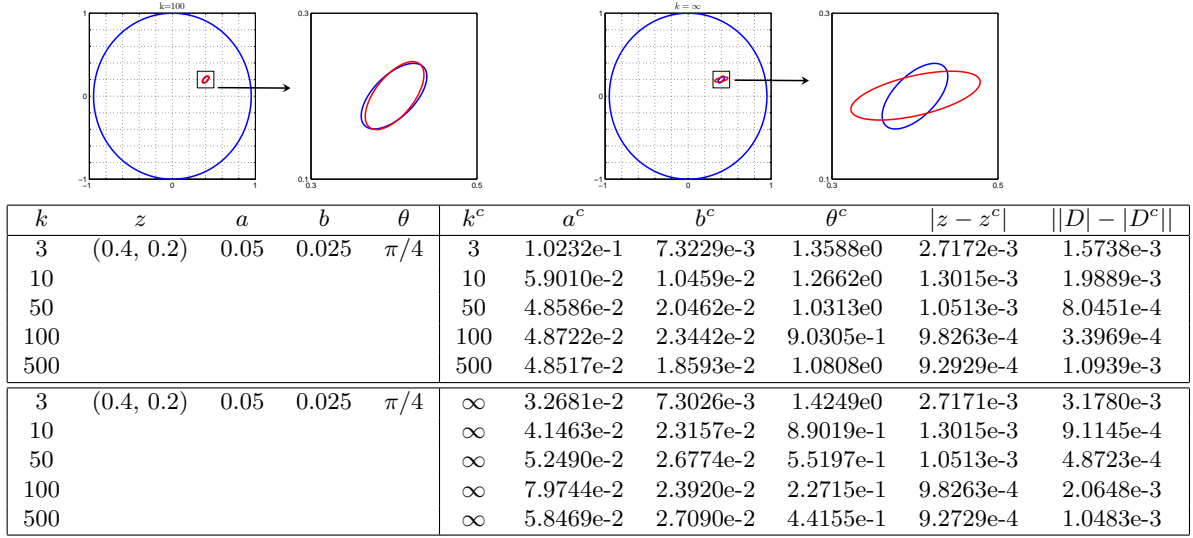


Figure 3: Reconstruction results when the inclusion is an ellipse. The red one is the detected ellipse.

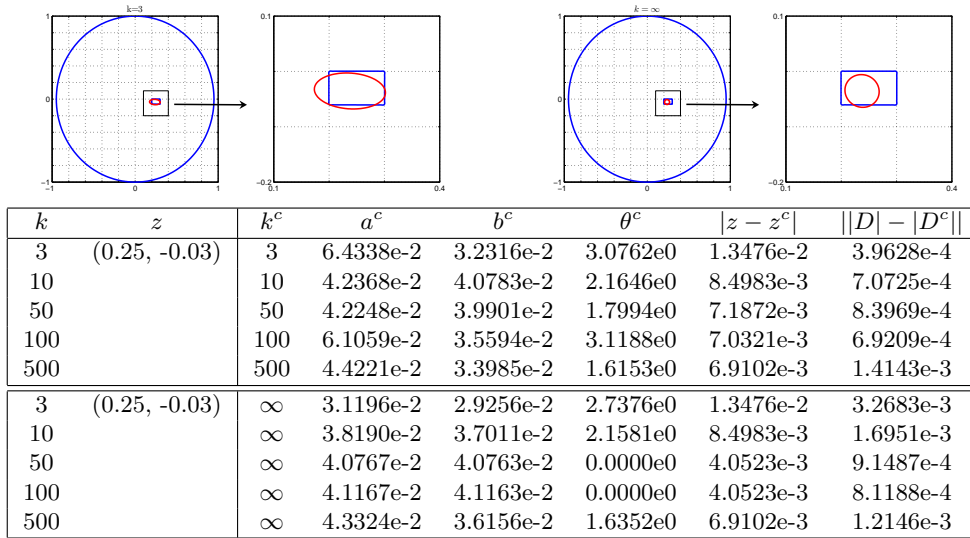


Figure 4: Reconstruction of an inclusion of general shape.

## 4 Conclusion

Based on a small volume expansion of the variations of the modal parameters that are due to the presence of a small inclusion, we have designed in this paper the first anomaly detection algorithm from modal measurements. Our algorithm consists on minimizing a functional

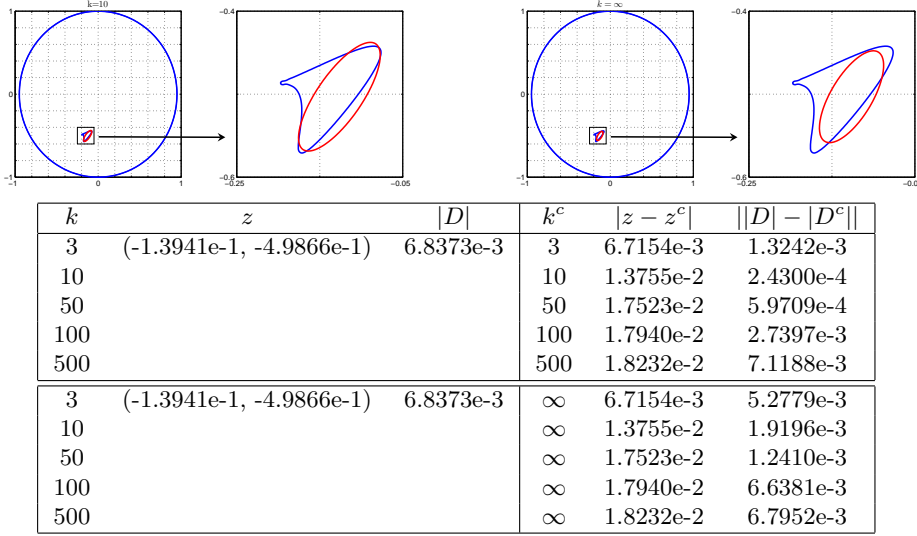


Figure 5: Reconstruction of an inclusion of general shape.

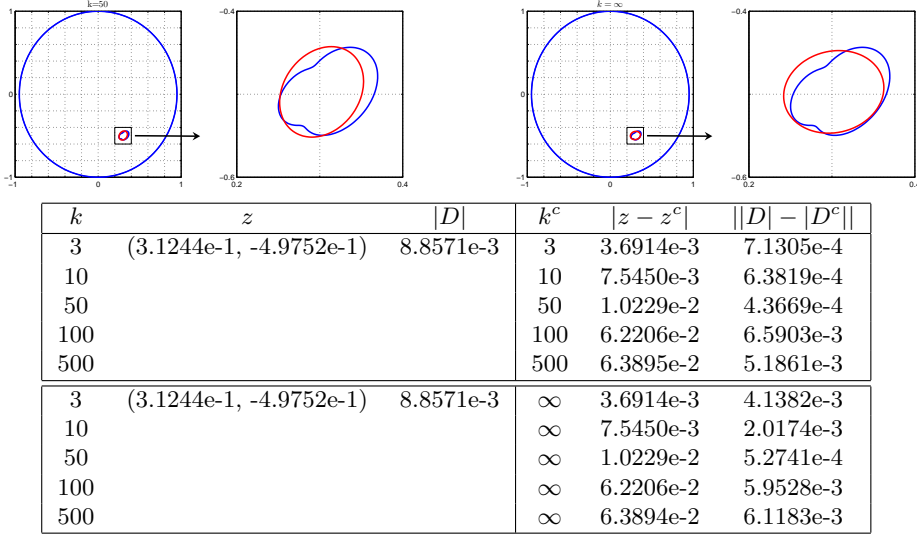


Figure 6: Reconstruction of an inclusion of general shape.

whose minimizer yields the location and the size of the anomaly. We have performed numerical experiments to test the viability of our algorithm. The results clearly demonstrate that the detection algorithm works well even the material parameter of the inclusion is not *a priori* known.

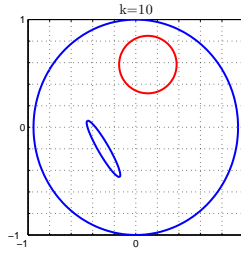


Figure 7: Reconstruction of an inclusion which is *not* small. Performance of algorithm is poor in this case.

## References

- [1] J. Albert, Generic properties of eigenfunctions of elliptic partial differential operators, *Trans. Amer. Math. Soc.*, 238 (1978), 341–354.
- [2] H. Ammari, Y. Capdeboscq, H. Kang, E. Kim, and M. Lim, Attainability by simply connected domains of optimal bounds for polarization tensors, *European Jour. of Applied Math*, 17 (2) (2006), 201–219.
- [3] H. Ammari and H. Kang, *Reconstruction of Small Inhomogeneities from Boundary Measurements*, Lecture Notes in Mathematics, Vol. 1846, Springer-Verlag, Berlin, 2004.
- [4] H. Ammari and H. Kang, *Polarization and Moment Tensors with Applications to Inverse Problems and Effective Medium Theory*, Applied Mathematical Sciences, Vol. 162, Springer-Verlag, New York, 2007.
- [5] H. Ammari, H. Kang, E. Kim, H. Lee, and K. Louati, Vibration analysis for detecting internal corrosion, submitted.
- [6] H. Ammari, H. Kang, and H. Lee, Asymptotic expansions for eigenvalues of the Lamé system in the presence of small inclusions, *Comm. Part. Diff. Equat.*, 32 (2007), 1715–1736.
- [7] H. Ammari, H. Kang, M. Lim, and H. Zribi, Layer potential techniques in spectral analysis. Part I : Complete asymptotic expansions for eigenvalues of the Laplacian in domains with small inclusions, preprint.
- [8] H. Ammari, H. Kang, G. Nakamura, and K. Tanuma, Complete asymptotic expansions of solutions of the system of elastostatics in the presence of an inclusion of small diameter and detection of an inclusion, *J. Elasticity*, 67 (2002), 97–129.
- [9] H. Ammari and S. Moskow, Asymptotic expansions for eigenvalues in the presence of small inhomogeneities, *Math. Meth. Appl. Sci.*, 26 (2003), 67–75.
- [10] G. Besson, Comportement asymptotique des valeurs propres du Laplacien dans un domaine avec un trou, *Bull. Soc. Math France* 113 (1985), 211–230.

- [11] M. Brühl, M. Hanke, and M. Vogelius, A direct impedance tomography algorithm for locating small inhomogeneities, *Numer. Math.*, 93 (2003), 635–654.
- [12] Y. Capdeboscq and M.S. Vogelius, A review of some recent work on impedance imaging for inhomogeneities of low volume fraction, *Partial differential equations and inverse problems*, 69–87, *Contemp. Math.* 362 (2004), Amer. Math. Soc., Providence, RI.
- [13] A. Friedman and M. Vogelius, Identification of small inhomogeneities of extreme conductivity by boundary measurements: a theorem on continuous dependence, *Arch. Rat. Mech. Anal.* 105 (1989), 299–326.
- [14] Z. Hashin and S. Shtrikman, A variational approach to the theory of the elastic behavior of multiphase materials, *J. Mech. Phys. Solids* 11 (1963), 127–140.
- [15] D. Jerison and N. Nadirashvili, The "hot spots" conjecture for domains with two axes of symmetry, *J. Amer. Math. Soc.*, 113 (2000), 741–772.
- [16] H. Kang, E. Kim, and J. Lee, Identification of Elastic Inclusions and Elastic Moment Tensors by Boundary Measurements, *Inverse Problems*, 19 (2003), 703–724.
- [17] H. Kang and G.W. Milton, On Conjectures of Polya-Szego and Eshelby, in *Inverse Problems, Multi-scale Analysis and Effective Medium Theory*, *Contemporary Math.* 408 (2006), 75–80.
- [18] H. Kang and G.W. Milton, Solutions to the Polya-Szego conjecture and the weak Eshelby conjecture, *Arch. Rational Mech. Anal.*, to appear.
- [19] T. Kato, *Perturbation Theory for Linear Operators*, Springer-Verlag, New York, 1976.
- [20] R. Kress, *Numerical Analysis*, Graduate Texts in Math., Vol. 181, Springer, 1998.
- [21] R. Lipton, Inequalities for electric and elastic polarization tensors with applications to random composites, *J. Mech. Phys. Solids*, 41 (1993), 809–833.
- [22] G. W. Milton, *The Theory of Composites*, Cambridge Monographs on Applied and Computational Mathematics, Cambridge University Press, 2002.
- [23] S. Ozawa, Singular variation of domains and eigenvalues of the Laplacian, *Duke Math. J.* 48 (1981), 767–778.
- [24] S. Ozawa, Electrostatic capacity and eigenvalues of the Laplacian, *J. Fac. Sci. Univ. Tokyo, Sect IA* 30 (1983), 53–62.
- [25] S. Ozawa, An asymptotic formula for the eigenvalues of the Laplacian in a three-dimensional domain with a small hole, *J. Fac. Sci. Univ. Tokyo, Sect IA* 30 (1983), 243–257.
- [26] K. Uhlenbeck, Generic properties of eigenfunctions, *Amer. J. Math.*, 98 (1976), 1059–1078.